Caractérisation expérimentale d'écoulements bouillants intervenant dans les récepteurs solaires à Génération Directe de Vapeur

Experimental characterization of boiling flows in Direct Steam Generation solar receivers

Israel AGUILERA-CORTES[1,2], Adrien TOUTANT[1,2] and Samuel MER[1,2*]

[1] Laboratoire PROcédés, Matériaux et Energie Solaire (PROMES-CNRS), Tecnosud, Rambla de la Thermodynamique – 66100 Perpignan France
[2] Université de Perpignan Via Domitia (UPVD), 52 Avenue Paul Alduy – 66100 Perpignan France
*(Corresponding author: samuel.mer@univ-perp.fr)

Résumé - Les technologies solaires thermiques à concentration (CST) concentrent le rayonnement solaire pour produire de la chaleur, utilisable pour l'électricité (CSP) ou l'industrie (SHIP). Les systèmes classiques utilisant des huiles ou sels fondus présentent des inconvénients, d'où l'intérêt pour la Génération Directe de Vapeur (GDV) dans les capteurs. Une boucle expérimentale, ConBo, a été conçue pour étudier l'écoulement bouillant eau-vapeur dans un tube, permettant de varier plusieurs paramètres et d'enregistrer les régimes d'écoulement. Les résultats ont montré un désaccord avec les corrélations existantes, conduisant au développement d'une nouvelle corrélation. L'analyse a aussi révélé que le haut du tube est souvent plus froid que le bas, un effet dû à la formation intermittente d'un film liquide améliorant le transfert thermique. Ces travaux visent à optimiser les récepteurs solaires pour la GDV.

Abstract - Concentrating solar thermal (CST) technologies concentrate solar radiation to produce heat, usable for electricity (CSP) or industry (SHIP). Conventional systems using oils or molten salts have drawbacks, hence the interest in Direct Steam Generation (DSG) within the collectors. An experimental loop, ConBo, was designed to study boiling water-steam flow in a tube, allowing several parameters to be varied and flow regimes to be recorded. The results showed a disagreement with existing correlations, leading to the development of a new one. The analysis also revealed that the top of the tube is often colder than the bottom, an effect due to the intermittent formation of a liquid film that improves heat transfer. This work aims to optimize solar receivers for DSG.

https://doi.org/10.25855/SFT2026-061

Nomenclature

A	area, m^2
Bo	Boiling number, $Bo = \dot{q}/(G\Delta h_{lv})$
C_0, C_1	empirical coefficients in Rouhani correlation
D	tube inner diameter, m
Fr	Froude number
G	mass flux, $\mathrm{kg/(s \cdot m^2)}$
H	dimensionless inlet subcooling, $H = (h_{\mathrm{in}} - h_{\mathrm{sat}})/\Delta h_{lv}$
h	heat transfer coefficient, $\mathrm{W/(m^2 \cdot K)}$
Δh_{lv}	latent heat of vaporization, $\mathrm{J/kg}$
k_l	liquid thermal conductivity, $\mathrm{W/(m \cdot K)}$
$\dot{m}$	mass flow rate, $\mathrm{kg/s}$
p	pressure, Pa
$\dot{q}$	heat flux, $\mathrm{W/m^2}$
$\dot{Q}$	electrical power supplied to inductor, W
Re	Reynolds number, $Re = GD/\mu_l$
s	sheltering coefficient (Jeffreys criterion)
T	temperature, K
ΔT_{sub}	inlet subcooling, K
u	velocity, $\mathrm{m/s}$
u^*	velocity ratio, u_s/u_l
x	vapor quality
X_{tt}	Martinelli parameter

Greek symbols

α	thermal diffusivity, $\mathrm{m^2/s}$
δ	liquid film thickness, m
ε	void fraction
θ	inclination angle, degrees
μ	dynamic viscosity, $\mathrm{Pa \cdot s}$
ν	kinematic viscosity, $\mathrm{m^2/s}$
ρ	density, $\mathrm{kg/m^3}$
σ	surface tension, $\mathrm{N/m}$

1. Introduction

The climate emergency underscores the need for sustainable energy alternatives. Concentrating Solar Thermal (CST) technologies are a viable solution, generating heat for electricity (CSP) or industry (SHIP) [9]. Conventional CSP plants use intermediary heat transfer fluids (HTFs) like oils or molten salts, which have drawbacks including environmental risks and high operational costs [14].

Direct Steam Generation (DSG) mitigates these issues by evaporating water directly within solar receivers, improving efficiency and reducing costs [8, 7]. However, DSG introduces complexities in managing two-phase water-steam flow, making accurate flow regime prediction essential [2]. Flow regimes dictate key thermal-hydraulic parameters like heat transfer coefficients and pressure drops. Foundational adiabatic studies established crucial models and flow pattern maps [4, 13, 16], later refined for boiling refrigerants [12, 5, 17]. Recent research has explored effects of complex geometries and non-uniform heat fluxes [1, 3, 18]. However, significant gaps persist concerning the combined influence of tube inclination, non-uniform heating, and flow regime transitions in boiling water at CSP-relevant scales.

This work introduces the ConBo experimental facility, designed to study convective boiling in a horizontal and slightly inclined tube representative of solar receivers. The study details an image processing technique for flow regime classification, analyzes the identified patterns, and reports on local heat transfer coefficients, providing data for DSG solar field design.

2. Materials and methods

2.1. Experimental set up

Figure 1 shows the ConBo facility, designed to investigate water boiling flows. It consists of three functional loops. In the main loop (salmon), water from a pressurized tank is pumped (up to 0.2 $\mathrm{kg/s}$) through a preheater and a 3-m establishment section before entering the 1-m test section. The Duplex steel test section (inner diameter 49.3 mm) is heated by induction.

The two-phase flow passes through a visualization box with a borosilicate glass tube for optical access. A secondary loop (green) thermalizes the visualization box to prevent condensation, and a cooling loop (blue) condenses the vapor.

The facility is comprehensively instrumented. Six high-precision PT100 sensors measure fluid temperature at different axial positions. Nine PT100 sensors on the external tube wall measure wall temperature at three axial stations (450, 750, 950 mm from inlet) and three circumferential positions (top, middle, bottom) each. Pressure is monitored with an absolute piezoelectric sensor, and a differential sensor measures the pressure drop across the boiling section.

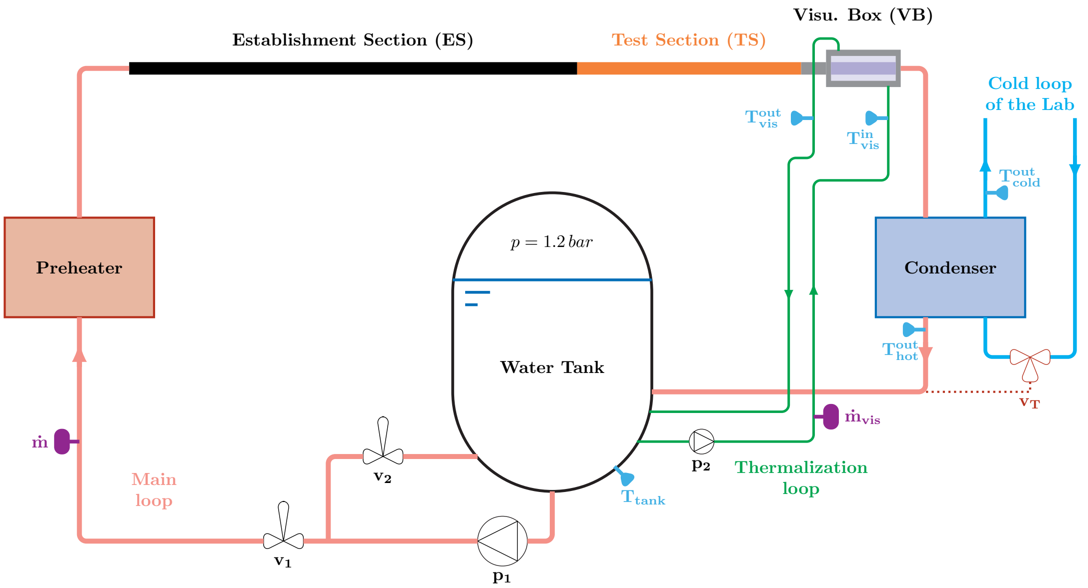

Figure 1 : *Schematic layout of the ConBo experimental facility.*

2.2. Image adquisition technique

A camera (*PROMON U1000*) acquired images at 151 fps. A 45° mirror positioned in front of the visualization box window minimized image distortion (Fig. 2). A `python` code using `OpenCV` processed the images through stages: preprocessing (vibration correction, rotation, cropping), correction (using a calibration pattern), processing (erosion, smoothing, normalization, binarization), and postprocessing to extract quantitative variables like vapor-phase velocity U_G and line void fraction $\varepsilon_{\text{line}}$.

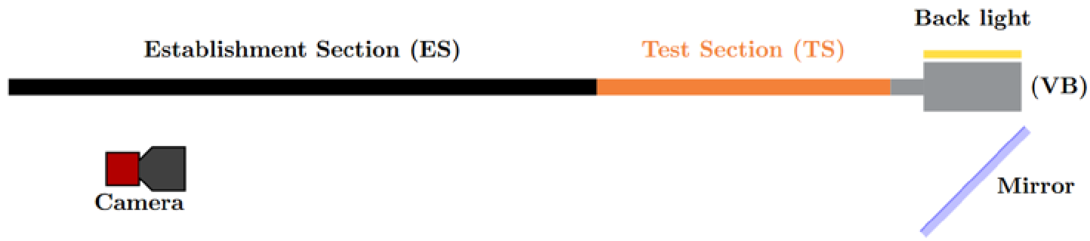

Figure 2 : *Top view scheme of the optical setup.*

2.3. Experimental procedure

Operating parameters (mass flow rate $\dot{m}$, inclination θ, inlet subcooling ΔT_{sub}, heater power $\dot{Q}$) were set. Data acquisition began once steady state was reached (temperature fluctuations within $\pm 0.5\,°\mathrm{C}$). Data was recorded for 60 s (temperatures, flow, inclination at 20 Hz; pressures at 67 Hz). Concurrently, a 7 s high-speed video (151 fps) was captured. The study includes 12 single-phase and 231 two-phase experiments. Conditions are summarized in Table 1.

Name	Fluid	n° points	G [kg/s·m²]	p [bar]	$\dot{q}$ [kW/m²]	x^{th} [%]	Configuration
Aguilera et al.	Water–steam	231	30–120	1.2	up to 100	from -1 to 5	0° and up to +5°

Table 1 : *Experimental conditions of Aguilera et al. dataset*

3. Results

3.1. Flow pattern classification

The 231 two-phase experiments were classified into four flow regimes: **Stratified (S)**, **Intermittent (I)**, **Smooth Stratified-Wavy (SW-S)**, and **Unstable Stratified-Wavy (SW-U)**. The patterns depend strongly on tube orientation (Fig. 3).

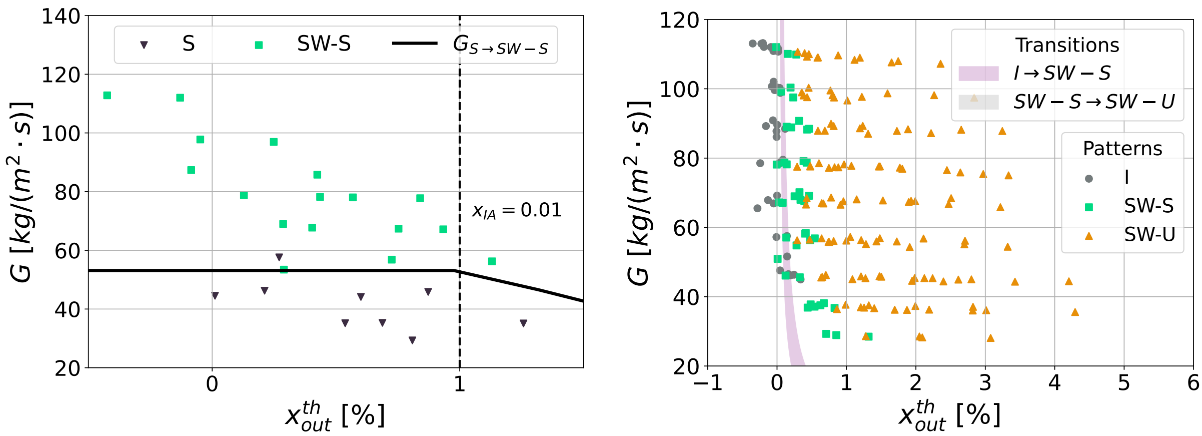

(a) Horizontal configuration ($\theta = 0°$).

(b) Inclined configuration.

Figure 3 : *Flow pattern classification. For horizontal flow, only S and SW-S patterns occur. Inclination eliminates S, introducing I and SW-U.*

For horizontal flow (Fig. 3a), the S to SW-S transition is governed by a modified Jeffreys criterion:

$$G_{S\rightarrow SW\text{-}S} = \left(\frac{4g\nu_l(\rho_l - \rho_v)\rho_l\rho_v}{s} \cdot \frac{\varepsilon^2(1-\varepsilon)}{x^2(1-x)} \right)^{1/3}, \quad (1)$$

where ε is from the Rouhani correlation [15]. To finalize the formulation of the transition, the inlet vapor quality x_{IA} from Kattan [12] has been used:

$$x_{\mathrm{IA}} = \left\{ \left[0.34^{1/0.875} \left(\frac{\rho_V}{\rho_L} \right)^{-1/1.75} \left(\frac{\mu_L}{\mu_V} \right)^{-1/7} \right] + 1 \right\}^{-1} \quad (2)$$

For inclined flows (Fig. 3b), transitions are controlled by void fraction ε. Experimental data show transition bands: $0.15 < \varepsilon_{I\rightarrow SW\text{-}S} < 0.25$ and $0.35 < \varepsilon_{SW\text{-}S\rightarrow SW\text{-}U} < 0.55$. These are captured by inverting the Rouhani correlation:

$$G = \frac{C_1(1-x)\left[g\sigma(\rho_L-\rho_V)\right]^{0.25}}{\rho_L^{0.5}\left[\frac{x}{\rho_V} - \varepsilon_{\text{band}}\left(1+C_0(1-x)\right)\left(\frac{x}{\rho_V}+\frac{1-x}{\rho_L}\right)\right]}, \tag{3}$$

with $C_0 = 0.12$. C_1 is empirically adjusted to 2 for the $I \rightarrow SW\text{-}S$ transition and to 3 for $SW\text{-}S \rightarrow SW\text{-}U$.

3.2. Heat transfer coefficients

Experimental heat transfer coefficients (HTCs) increase along the flow direction and with vapor quality, with the SW-U regime yielding the highest values. Existing correlations [6, 11, 10] fail to accurately predict the data, as they were developed for refrigerants in smaller geometries and rely on the Martinelli parameter, unsuitable for the low vapor qualities here.

A new correlation was developed by modifying Fang et al.'s model [6]:

$$h_{\text{theo}} = \frac{k_l}{D} Bo\, Re^{1.6}\left(x^{th} - H\right)^{0.8}\left[\ln\left(\frac{\mu_{lf}}{\mu_{lw}}\right)\right]^{-1.55} \tag{4}$$

where $Bo = \dot{q}/(G\Delta h_{lv})$, $Re = GD/\mu_l$, $H = (h_{\text{in}} - h_{\text{sat}})/\Delta h_{lv}$, μ_{lf} and μ_{lw} are liquid dynamic viscosities at fluid and wall temperature.

The new correlation shows excellent agreement (Fig. 4), with a mean absolute percentage error (MAPE) of 10.43% and 96.9% of data within ±30% error.

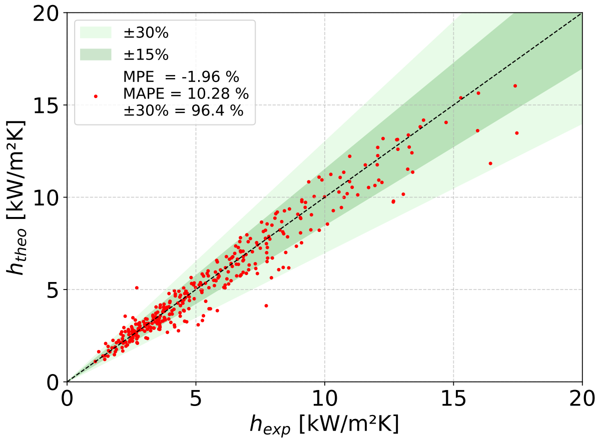

Figure 4 : *Comparison between experimental heat transfer coefficients and the proposed new correlation.*

3.3. Cross-sectional temperature difference

In horizontal two-phase flow, phase separation typically leads to $T^{\text{top}} > T^{\text{bot}}$ due to the lower vapor heat transfer coefficient. However, our data show the opposite ($T^{\text{top}} < T^{\text{bot}}$, up to -15 K in section S_3). This is attributed to intermittent formation of a thin liquid film on the upper wall, formed by waves or associated to large bubble passage on the upper part of the tube, enhancing local heat transfer.

A mechanistic model explains this behavior. The heat transfer coefficients for the upper film ($h_{\text{cb}}^{\text{top}}$) and lower liquid ($h_{\text{cb}}^{\text{bot}}$) are estimated using respectively the Kattan and Dittus Boelter correlations:

$$h_{\text{cb}}^{\text{top}} = 0.0133\,\text{Re}_{\delta_{\text{top}}}^{0.69}\text{Pr}_l^{0.4}\frac{k_l}{\delta_{\text{top}}}, \quad h_{\text{cb}}^{\text{bot}} = 0.023\,\text{Re}_{D_{\text{in}}}^{0.8}\text{Pr}_l^{0.4}\frac{k_l}{D_{\text{in}}} \tag{5}$$

where δ_{top} is the upper liquid film thickness. The ratio $h^* = h_{\text{cb}}^{\text{top}}/h_{\text{cb}}^{\text{bot}}$ increases with velocity ratio $u^* = u_s/u_l$ and decreasing film thickness. A time-averaged ratio h_{avg}^* is calculated based on the film wetting period t_{film} and cycle time t_{cycle}:

$$h_{\text{avg}}^* = 1 + \frac{t_{\text{film}}}{t_{\text{cycle}}}(h^* - 1) \tag{6}$$

The theoretical temperature difference is:

$$T^{\text{top}} - T^{\text{bot}} \approx \frac{\dot{q}}{h_{\text{cb}}^{\text{bot}}}\left(\frac{1 - h_{\text{avg}}^*}{h_{\text{avg}}^*}\right) \tag{7}$$

Figure 5 shows good agreement between model predictions and experimental data for intermittent flow for which the only model variable to adjust is δ_{top}.

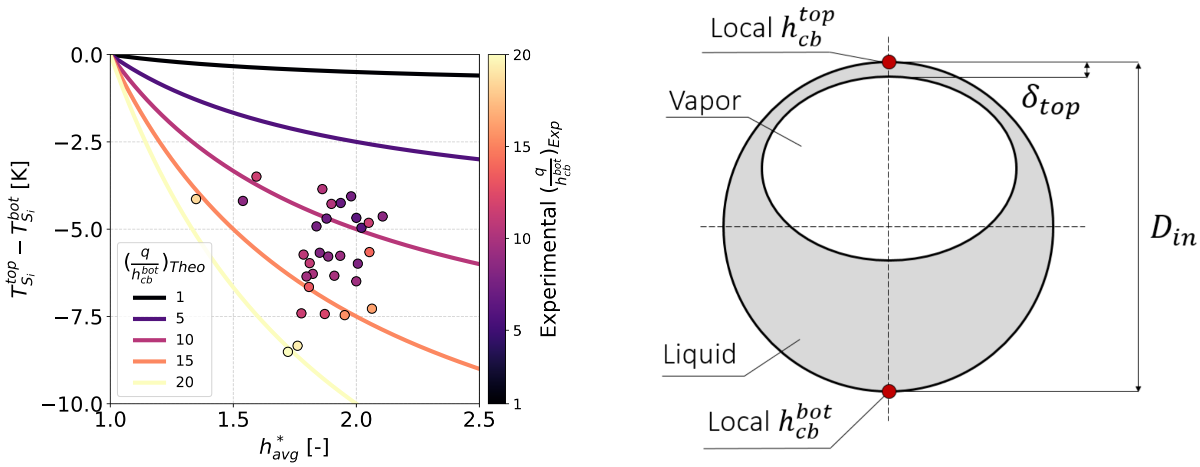

(a) Theoretical lines and experimental points. (b) Schematic of the liquid film thickness.

Figure 5 : *Comparison of theoretical and experimental temperature differences for intermittent flow, considering* $\delta_{top} = 0.004 \cdot D_{in} \approx 0.2\,mm$.

4. Conclusion

An experimental study of boiling water-steam flow in a horizontal and slightly inclined tube representative of DSG solar receivers has been conducted. Flow pattern maps for both horizontal and inclined configurations were established, identifying four distinct regimes and demonstrating the dominant role of void fraction in transition criteria for inclined flows.

The analysis of local heat transfer coefficients revealed that existing correlations, developed primarily for refrigerants, are inadequate for predicting the present data. Consequently, a new, dimensionally consistent correlation was proposed, achieving excellent agreement with experimental results (MAPE of 10.43%).

Furthermore, the study identified a counter-intuitive circumferential temperature distribution, where the top of the tube is often colder than the bottom. A mechanistic model, based on the intermittent formation of a thin liquid film on the upper wall, was developed and successfully validated against experimental data for intermittent flows.

These results provide valuable insights and reliable tools for the thermal-hydraulic design and optimization of Direct Steam Generation solar receivers, contributing to the advancement of more efficient and sustainable concentrating solar power systems.

5. References

[1] A. Araújo et al.. 2024 *"Heat transfer characteristics of horizontal flow boiling with uniform and non-uniform circumferential heat flux" International Journal of Heat and Mass Transfer*, 228

[2] A. Aurousseau et al.. 2016 *"Control systems for direct steam generation in linear concentrating solar power plants – A review" Renewable and Sustainable Energy Reviews*, 56

[3] J. Dirker et al.. 2022 *"The effect of circumferentially non-uniform heat flux on flow boiling heat transfer in a horizontal tube" International Journal of Heat and Mass Transfer*, 185

[4] A. E. Dukler and M. G. Hubbard. 1975 *"A Model for Gas-Liquid Slug Flow in Horizontal and Near Horizontal Tubes" Industrial & Engineering Chemistry Fundamentals*, 14

[5] J. El Hajal et al.. 2003 *"Condensation in horizontal tubes, part 1: Two-phase flow pattern map" International Journal of Heat and Mass Transfer*, 46

[6] X. Fang et al.. 2017 *"A general correlation for saturated flow boiling heat transfer in channels of various sizes and flow directions" International Journal of Heat and Mass Transfer*, 107

[7] A. Fernández-García et al.. 2010 *"Parabolic-trough solar collectors and their applications" Renewable and Sustainable Energy Reviews*, 14

[8] A. Giglio et al.. 2017 *"Direct steam generation in parabolic-trough collectors: A review about the technology and a thermo-economic analysis of a hybrid system" Renewable and Sustainable Energy Reviews*, 74

[9] M. T. Islam et al.. 2018 *"A comprehensive review of state-of-the-art concentrating solar power (CSP) technologies: Current status and research trends" Renewable and Sustainable Energy Reviews*, 91

[10] J. S. Jabardo et al.. 1999 *"New correlation for convective boiling of pure halocarbon refrigerants flowing in horizontal tubes" Braz. J. Mech. Sci*, 21

[11] S. G. Kandlikar. 1990 *"A general correlation for saturated two-phase flow boiling heat transfer inside horizontal and vertical tubes" Journal of Heat Transfer*, 112

[12] N. Kattan et al.. 1998 *"Flow boiling in horizontal tubes: Part 1 – Development of a diabatic two-phase flow pattern map" Journal of Heat Transfer*, 120

[13] J. M. Mandhane et al.. 1974 *"A flow pattern map for gas–liquid flow in horizontal pipes" International Journal of Multiphase Flow*, 1

[14] *NREL Database: Andasol 1 CSP Project - Powerplant details*. 2022.

[15] S. Z. Rouhani and E. Axelsson. 1970 *"Calculation of void volume fraction in the subcooled and quality boiling regions" International Journal of Heat and Mass Transfer*, 13

[16] Y. Taitel and A. E. Dukler. 1976 *"A model for predicting flow regime transitions in horizon and near horizontal gas-liquid flow" AIChE Journal*, 22

[17] L. Wojtan et al.. 2005 *"Investigation of flow boiling in horizontal tubes: Part I – A new diabatic two-phase flow pattern map" International Journal of Heat and Mass Transfer*, 48

[18] L. Yin et al.. 2014 *"Experimental study on flow boiling of water in small-diameter horizontal tubes with U-shaped configurations" Chemical Engineering Science*, 104